applied sciences

MDPI

Article

Tribological Properties of Two Typical Materials of Hydraulic Motor's Rotor at Different Ambient Temperatures

Gao Wan [1,2], Qing Wu [1,*], Min Tang [3,4,*], Mingjian Lu [3,4,*] and Kun Yang [1,2]

[1] School of Transportation and Logistics Engineering, Wuhan University of Technology, Wuhan 430063, China; wangao@whut.edu.cn (G.W.); kyang@whut.edu.cn (K.Y.)
[2] Reliability Engineering Institute, National Engineering Research Center for Water Transportation Safety, Wuhan 430063, China
[3] National Engineering Research Centre for Water Transport Safety, Wuhan University of Technology, Wuhan 430063, China
[4] Intelligent Transportation Systems Research Center, Wuhan University of Technology, Wuhan 430063, China
* Correspondence: wq@whut.edu.cn (Q.W.); tangmin@whut.edu.cn (M.T.); mingjian_lu@whut.edu.cn (M.L.)

Abstract: Cold starting is the biggest challenge for mechanical equipment in polar environments. Selecting suitable friction pair materials and exploring the wear mechanism are keys to improving the reliability in a low-temperature environment. This study analyzed the tribological properties of the two typical materials of hydraulic motor's rotor at different ambient temperatures, especially at low temperature. Finally, it explored the wear process and mechanism of two sets of friction pairs. The results showed that the low temperature environment not only affects the viscosity of the hydraulic medium in the hydraulic system and changes the lubrication state between the friction pairs, but also enhances the cold brittleness of metal materials and affects the wear characteristics between the friction pairs. There is a maximum difference of around −20 °C. The wear volume of material QT500-7 sharply increases and reaches a maximum of 0.107 mm^3 when the normal force is 20 N, which is 3.65 times as much as the wear volume of the LC2-1. When the normal force is 30 N, the wear volume of materials QT500-7 and LC2-1 are 0.125 and 0.036 mm^3, respectively. The wear volume of the former is 3.4 times that of the latter. In addition, it indicates that the impact energy of the material affects its tribological properties since the impact energy of the material QT500-7 decreases sharply, including two consecutive subintervals of sharp decreases from 97.3 J to 42.2 J and then to 18.0 J at the temperature of −10 to −30 °C. The material LC2-1 with stable wear performance is more applicable for being processed and manufactured into parts for low-temperature environmental conditions, as there is no serious fluctuation in the temperature range from −40 °C to room temperature. The research findings are expected to provide a theoretical support for hydraulic motors design, material selection and the maintenance of polar deck machinery. They are of great significance for improving the operational reliability of hydraulic motors for polar ships.

Keywords: polar vessel; hydraulic vane motor; low-temperature wear; tribological characteristics; cold starting

Citation: Wan, G.; Wu, Q.; Tang, M.; Lu, M.; Yang, K. Tribological Properties of Two Typical Materials of Hydraulic Motor's Rotor at Different Ambient Temperatures. *Appl. Sci.* **2022**, *12*, 5582. https://doi.org/10.3390/app12115582

Academic Editors: Carter Hamilton, Xinyi Xiao and Hanbin Xiao

Received: 12 May 2022
Accepted: 28 May 2022
Published: 31 May 2022

1. Introduction

The Arctic region has entered a preparatory period for development and exploitation, and its value has become increasingly prominent in terms of resources, transportation and geostrategy [1]. The average winter temperature in the polar regions is about −40 °C, with the daily mean temperature reaching −53 °C under extreme conditions. Polar vessel equipment is the basis and guarantee for the accomplishment of polar scientific investigations and polar development. In extremely cold climate, polar transportation and deck machinery of engineering ships run into many operational problems due to the low temperature [2].

The ambient temperature has a certain effect on most friction systems [3,4]. As the actuator, the hydraulic motor is exposed to the polar low temperature environment for a long time; the physical and chemical properties of the hydraulic oil change dramatically and respond fastest to temperature change, which directly affects the lubrication state [5,6] and then causes the change of the wear state [7]. The research results discovered by Bergada [8] showed that the average oil film thickness decreased with the increase in hydraulic oil temperature and pump outlet pressure. Tang [9] established a thermal elastohydrodynamic lubrication model for a slipper pair of axial piston pumps by considering the elastohydrodynamic characteristics of hydraulic oil and the coupling effect of the visco-temperature effect, and derived the deformation of the slipper and distribution law of oil film thickness, pressure, and temperature. The results indicate that the slipper surface elastic deformation is affected by the local pressure peaks, which enhances the elasto-hydrodynamic effect, and the oil film temperature is strongly dependent on the film thickness. With a decrease in film thickness, the film temperature becomes higher due to the increase in viscous friction in the film gap. Wang [10] analyzed the relationship between temperature, rolling speed, and sliding speed and the friction coefficient of the oil on a self-developed friction testing machine simulating aerospace bearings. The results show that its viscosity varies considerably when the temperature is below 0 °C, and its viscosity varies slowly when the temperature is above 30 °C. When the sliding speed is less than 0.3 m/s, the friction coefficient of this oil varies linearly with the sliding speed. When the sliding speed surpasses 0.3 m/s, the friction coefficient varies nonlinearly with the sliding speed. When the sliding speed surpasses 1 m/s, the friction coefficient remains about the same with the increase in sliding speed.

The ambient temperature can affect not only the characteristics of the lubricating medium, but also the mechanical properties of metal materials [11–13], thereby affecting the wear characteristics [14,15]. Some scholars [16–20] have studied the properties of metallic material at low temperature by mechanical experiments and material preparation methods. Extreme temperatures could cause the degradation of various metallic material properties, such as strength and toughness, before the formation of macroscopic cracks, thereby affecting the tribological properties of friction pair services [21–23]. Jaswin [24] conducted experimental research to improve the wear resistance of two kinds of valve steels through shallow and deep cryogenic treatment. Additionally, some researchers [7,25] have studied the metallic material tribology in a low-temperature environment using a testing machine. The experimental results showed that the low-temperature environment had a great impact on the frictional performance of materials. Wang [26,27] indicated that temperature could change the wear pattern between friction pairs. These articles revealed that when the ambient temperature was 20 °C, the main forms of 10CrMn2NiSiCuAl suffered fatigue damage, oxidative wear, and adhesive wear. However, when the temperature dropped to −20 °C, desquamation and spherical wear debris appeared on the worn surface, which rapidly increased the wear rate. Wang [28] showed that as the temperature decreased, the weakening of the oxidation of the wear debris became a dominant reason for the increase in wear and the reduction in oxides in the debris increased the adhesion between the two metals. Ma [29,30] studied the rolling contact fatigue damage behavior of high-speed railway wheel materials under non-lubricated conditions at room temperature and low temperature, respectively. The results showed that the wear rate, plastic deformation, and fatigue damage of the wheel materials were all significantly higher in the low-temperature environment than in the room-temperature environment. The form of wear changed from oxidative wear and abrasive wear into fatigue and adhesive wear.

Although different scholars have made many achievements in the research on the influence of temperature on friction and wear of friction pairs and wear mechanism, there are still many aspects to be further deepened in the research on the friction and wear performance of friction pairs of marine hydraulic motors in a polar or low-temperature environment. Nevertheless, research remains limited regarding the performance of metallic materials, especially of those for hydraulic vane motors used in a low-temperature environment.

Compared to ordinary ship deck machinery, various deck equipment on polar ships are required to have better low-temperature resistance. Hydraulic motors in deck machinery are no exception. Cold starting is the biggest challenge to deck machinery in the open air under polar conditions [31]. In the process of cold starting, the internal temperature of the motor undergoes a dynamic changing process in which the temperature of the hydraulic oil is defended from low temperature to high temperature but in which the temperature of the internal parts cannot change directly from low to high. During cryogenic operation, low temperature affects material properties and enhances the cold brittleness of metal materials. The abnormal wear of internal parts is commonplace and leads to equipment damage or even operational troubles [32]. In view of the above reasons, it is imperative to select materials applicable for cold climates and analyze the wear mechanism under extreme temperature conditions.

2. Materials and Methods

2.1. Materials

The experimental object in this study is the HNM-STS type vane hydraulic motor (Figure 1a), which is widely used on ships. The motor's internal rotation mechanism is mainly composed of vanes, a rotor, a distribution plate, a motor shell and other parts. When the high-pressure oil is charged into the motor, the two vanes drive the rotor to rotate due to different areas of action and the formation of a rotation torque. During the operation of the hydraulic motor, due to the unbalanced pressures on both sides of the rotor, the generated pressure pushes the rotor to slide toward and relative to the distribution plate so that the surface of the distribution plate and the rotor are worn (Figure 1b). As the leakage of the hydraulic motor increases, so do the unbalanced pressures on both sides, which further aggravates the wear condition of the rotor and the distribution plate and reduces the working efficiency and service life of the hydraulic motor.

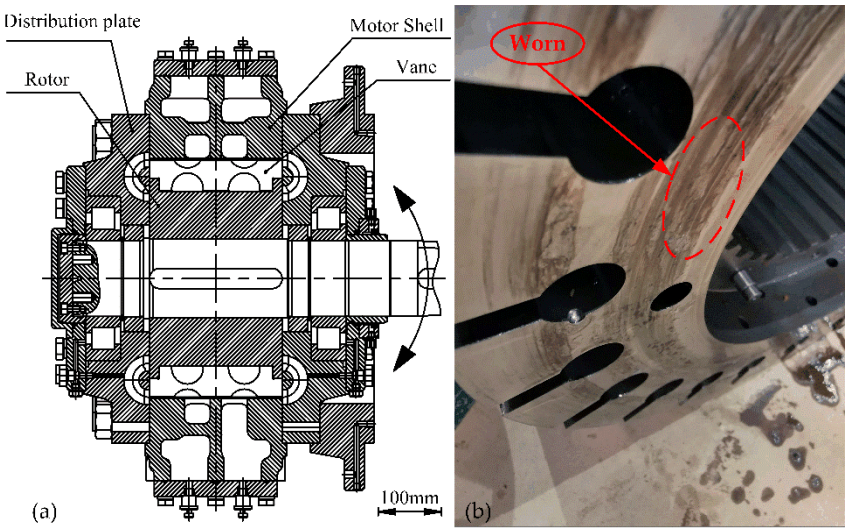

Figure 1. (**a**) The HNM-STS type vane hydraulic motor; (**b**) the worn surface of the rotor.

Two types of metallic materials, QT500-7 (GB/T1348-2009) and LC2-1 (JB/T 724 8-2008), can be used to make cryogenic valves and hydraulic components. In this study, these materials were processed into pin samples. The material QT350-22L (ISO 1083:2004), which was determined to be a distribution plate, was processed into disc samples. The pins and discs had distinct diameters of 20 mm and 30 mm and distinct heights of 20 mm and 8 mm, respectively. The chemical compositions of the sample materials are shown in Table 1. The surfaces of the samples were polished before the test. The surfaces of the pins and discs were polished using an automatic positioning arc polishing machine (YH2M8690, YUHUAN CNC MACHINE TOOL Co., Ltd., Changsha, China) and sand paper. The paper that is 400 mesh, 800 mesh, 1200 mesh, and 2000 mesh and the corresponding polishing

agent were used on a step-by-step basis. After polishing, the surface roughness of each sample was measured by confocal laser scanning microscope (CLSM) (VK-2000, KEYEBCE, Osaka, Japan). The roughness (Ra) of the sample materials measured 0.4 ± 0.05 μm. The schematic data are shown in Figure 2.

Table 1. Chemical compositions of pin and disc samples.

	Chemical Compositions (%)					
	C	**Si**	**Mn**	**P**	**S**	**Ni**
QT350-22L	≤3.67	≤2.58	≤0.560	≤0.032	≤0.022	≤0.013
LC2-1	≤0.25	≤0.60	0.50~0.80	≤0.04	≤0.045	2.0~3.0
QT500-7	3.55~3.85	2.34~2.86	≤0.6	≤0.08	≤0.025	~

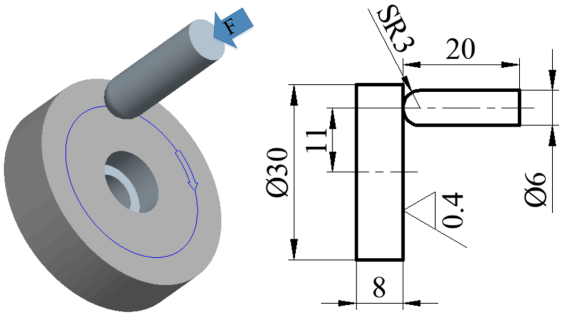

Figure 2. Test samples and schematic data of sliding wear testing.

2.2. Hydraulic Oil

The viscosity of oil varies dramatically depending on the temperature difference. As the viscosity of the lubricant changes, the lubrication characteristics between the friction pairs also change. So, the lubrication effect is non-negligible in this study. Low-temperature hydraulic oil usually has good wear resistance, low-temperature fluidity, shear resistance, and low-temperature start performance, and in long-term low-temperature storage will not form precipitation, turbidity, and stratification, and has long service life. The 15# aviation hydraulic oil (GJB 1177-1991, Petro China Yumen Oilfield Company, Jiuquan, China) is mainly used in the transmission mechanism of aerospace hydraulic equipment and the working medium of large ship lifting. It can be used in the transmission equipment of ship deck machinery in extremely cold regions. Therefore, this paper chooses this type of aviation hydraulic oil as the test sample. The steady-state rheological test was carried out using the MCR 102 rotary rheometer(MCR 102, Anton Pear, Graz, Austria). In this test, the rotation mode was selected, and the shear rate was set at 600 r/min.

The purpose of the experiment in this paper is mainly aimed at the tribological properties of the friction pair composed of two materials in the process of cold starting at different temperatures, especially cold starting at low temperature. Meanwhile, a set of starting tests at room temperature are set up for comparative tests. Therefore, six temperatures (room temperature (25 °C), 0 °C, −10 °C, −20 °C, −30 °C, and −40 °C).

2.3. Material Properties Experiments

Generally, temperature has an impact on the mechanical properties of all metals. Compared with the effect of high-temperature conditions on material mechanics, the most intuitive effect of low-temperature conditions is the hardness and strength of the material. Brittleness are unique ones among these properties. The change in mechanical properties of the material will also affect the wear performance of the friction pair material.

The impact strength of the materials in this paper was tested according to the standard of the Metallic materials-Charpy pendulum Impact Test Method (GB/T 229-2007 or ISO 148-1:2006). All impact strength tests were performed on a pendulum impact testing ma-

chine (ZBC2302-B, MTS, Shenzhen, China) with a standard impact energy of 300 J. Test samples are also based on standard samples. The samples were installed in a low-temperature environment box, where the temperature was turned down to the corresponding temperature range at a certain cooling rate, with an error maintained at less than ±1 °C for at least 30 min.

In order to reduce test errors caused by material defects or other factors, each ground test was performed three times according to the test standard. Samples of the same material were tested three times at room temperature (25 °C), 0 °C, −10 °C, −20 °C, −30 °C and −40 °C, respectively. The average value of the three tests is the impact energy value of the material at this temperature. The impact test bench, sample, and the installation diagram of impact test sample are shown in Figure 3.

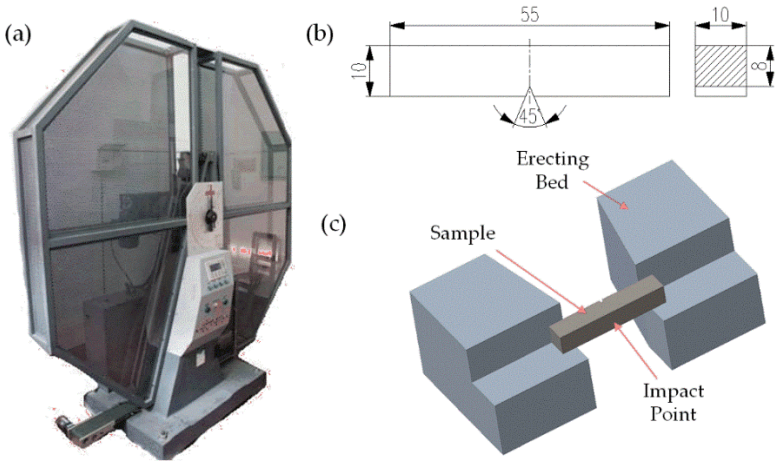

Figure 3. (**a**) Impact testing machine (ZBC2302-B). (**b**) Sample. (**c**) Impact sample installation diagram.

2.4. Experimental Methods of Tribological Properties

All of the tribological experiments were conducted using a testing machine (3 KW testbed, Wuhan University of Technology, China, as shown in Figure 4) to determine the tribological properties of LC2-1 and QT500-7 sliding contact on QT350-22L in a low-temperature hydraulic oil environment. The wear track of the pins after experiments was observed and measured using CLSM, while the wear surface was investigated using scanning electron microscope (SEM) (VEGA3, TESCAN, Brno, Czech Republic). The wear volume was calculated based on the measured results using the integral principle. A microscope (BX3M, Olympus, Tokyo, Japan) and a ferrography analyzer were used to observe and analyze the wear particles in the oil, respectively, after the test.

As shown in Figure 4, a low-temperature cavity (5) was fixed on the testbed to provide a low-temperature environment. The disc (11) and pin (12) were installed at the front of the rotating axle (4) and the axle (6) by using fixtures, respectively. Hydraulic oil was injected into the house through the flow path on the axle (6). Low-temperature equipment (FP89-HL, Julabo, Seelbach, Germany offered the circulating cooling medium to copper tube (9) installed in the cavity's interior. The circulating cooling medium came into and out of the cavity through the oil ports (14 and 16). The refrigerant was impelled by the compressors to recirculate in the copper tube to cool the coolant (10), which provided a low-temperature environment in the cavity. A digital temperature sensor (13) was fixed into the cavity to monitor the temperature in real time. The temperature signal collected is directly transmitted to the temperature control system of the refrigerator, forming a closed-loop control of temperature. The temperature of the hydraulic oil in the low-temperature oil chamber was real-time controlled. During the experiment, the low temperature was kept stable with a fluctuation of less than 1 °C.

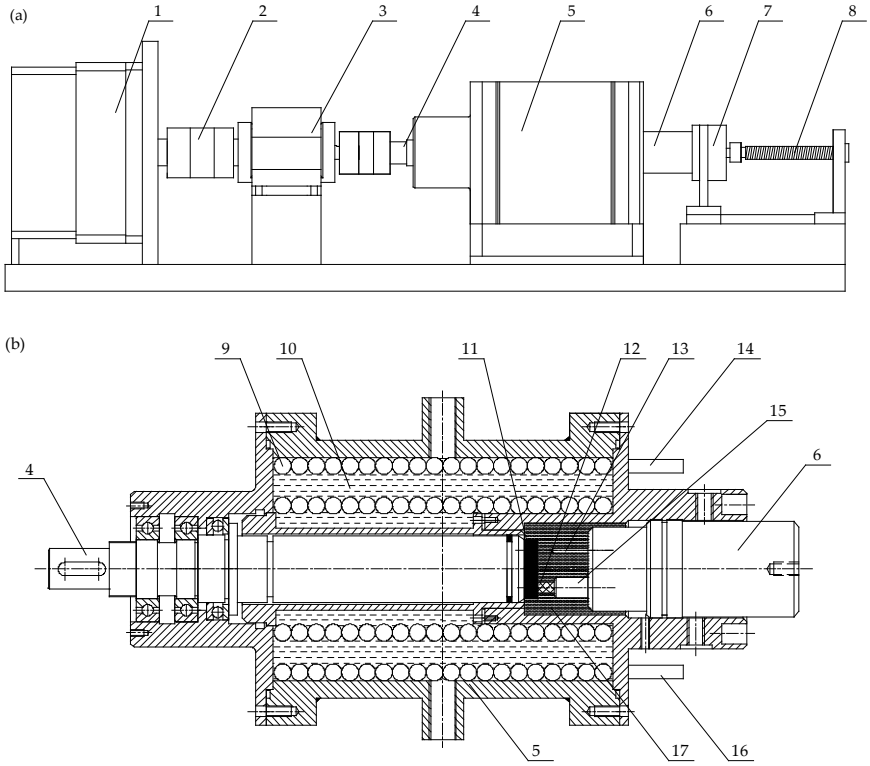

Figure 4. (**a**) The testing machine system and the physical map; (**b**) schematic diagram of the internal structure of the low-temperature cavity.1—converter motor; 2—couplings; 3—torque sensor; 4—rotation axle; 5—low-temperature cavity; 6—axle; 7—loading sensor; 8—loading screw; 9—copper tube; 10—coolant; 11—the disc sample; 12—the pin sample; 13—temperature sensors; 14—outlet of coolant; 15—the fixture of pin; 16—inlet of coolant; 17—the tested hydraulic oil.

The testing machine was driven by a converter motor (1) whose rotary speed was controlled by a frequency conversion controller. The axle was pushed to slide by loading screw (8) compression spring so that the pin was pressed against the surface of the disc. The normal force was detected by a loading sensor (7). Meanwhile, a torque sensor (3) (measurement error: ±2%) was employed to measure tangential torque. The data of the normal force, the tangential force and the temperature could be recorded automatically on the computer.

The entire wear test was divided into 24 groups. The experiments were performed at room temperature (25 °C), 0 °C, −10 °C, −20 °C, −30 °C and −40 °C, respectively. During the test, the ambient temperature was always kept stable. In addition, the normal force was set to 20 N and 30 N, respectively, to study its influence on the two typical materials. The rotary speed of the converter motor was 300 r/min^{-1}. The experiments were carried out under each frictional condition for 120 min. The test plan is shown in Table 2.

Table 2. Related parameters of the test plan.

Test Conditions		**Temperature/°C**					
		(Rotary Speed 300 r/min; 120 min)					
Normal force	20 N	25	0	−10	−20	−30	−40
	30 N						

The center line of the pin was located 11 mm eccentrically from the center line of the disc. The coefficient of friction was measured and calculated using the following Equation (1):

$$f = T/(0.011 * N) \quad (1)$$

In this equation, f is the coefficient of friction; T is the friction torque (N·m), which was employed by the torque sensor (3); and N is the normal force (N), which was detected by the loading sensor (7).

3. Results

3.1. Mechanical Properties

As shown in Figure 5, the impact energy of the two types of materials decreases as temperature decreases. The impact energy of LC2-1 decreases from 127.7 J to 21.6 J as the temperature falls from 25 °C to −40 °C. The sharpest decrease occurs within the temperature ranges from −30 °C to −40 °C. The amplitude of change is −26.3 J, or −54.8% in percentage. For the material QT500-7, as the test temperature drops from 25 °C to −40 °C, its impact energy drops from 141.7 J to 13.3 J, including two consecutive subintervals of sharp decreases from 97.3 J to 42.2 J and then to 18.0 J as the temperature drops from −10 °C to −20 °C and then to −30 °C. The percentage decreases are −56.6% and −57.3%, respectively. In addition, the impact energy continues decreasing as the temperature decreases. It is worth mentioning that the brittle–ductile transition temperature of QT500-7 ranges from −10 °C to −30 °C. To sum up, the results indicate that the fracture ability of the materials worsens, while the brittleness increases as the temperature drops. The variation trend of the impact energy of LC2-1 is not as obvious as that of QT500-7.

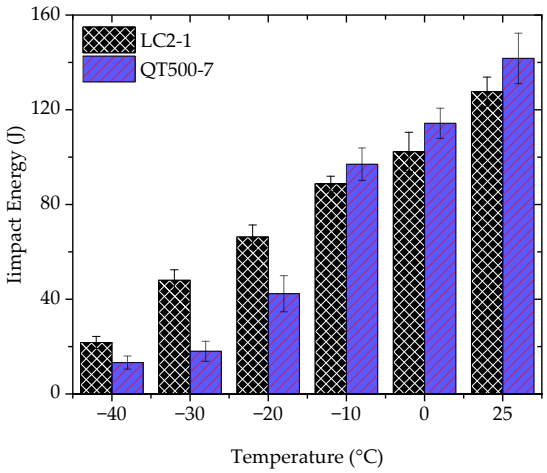

Figure 5. Variations of impact energy of the material with temperature.

3.2. Coefficient of Friction

As shown in Figure 6, the coefficients of friction of two sets of friction pair LC2-1/QT350-22L and QT500-7/QT350-22L have an obvious variation trend under various conditions. In addition, the viscosity has also been taken into consideration and varies obviously. As the test temperature drops, the oil viscosity increases and the viscosity gradient increases. As the test temperature drops from 25 °C to −40 °C, the viscosity of hydraulic oil increases from 15.96 to 263.27 mPa·s. The viscosity gradient increases with the temperature dropping. The minimum gradient of the oil viscosity with temperature is 0.71 mPa·s/°C when the test temperature ranges from 25 °C to 0 °C. The viscosity of the hydraulic oil is 147.73 to 263.27 mPa·s when the temperature drops from −30 °C to −40 °C, and there is the maximum viscosity gradient and it is 11.95 mPa·s/°C. The viscosity gradient is increased by about 16.8 times.

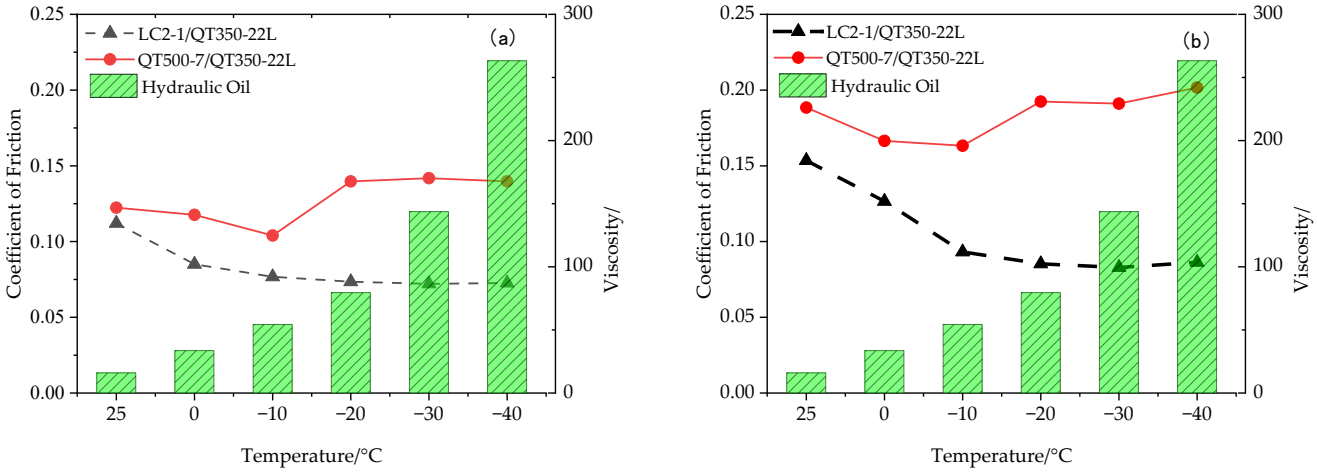

Figure 6. Coefficient of friction curves of LC2-1/QT350-22L and QT500-7/QT350-22L. (**a**) The normal force is 20 N. (**b**) The normal force is 30 N.

As shown in Figure 6a, the normal force is 20 N. At room temperature (25 °C), the coefficients of friction of the friction pairs LC2-1/QT350-22L and QT500-7/QT350-22L are relatively close, about 0.1201, indicating that the wear performance of the two sets of friction pairs is similar at room temperature. When the test temperature is −10 °C, the coefficients of friction of the two sets of friction pairs both decrease. The coefficient of friction of the former is about 0.0771, and the coefficient of friction of the latter is about 0.1021. The coefficient of friction of the former has a bigger decreasing rate than does that of the latter. When the test temperature is −20 °C or less, the coefficient of friction of the friction pair LC2-1/QT350-22L is basically stable at about 0.0753. However, the coefficient of friction of the friction pair QT500-7/QT350-22L increases significantly at −20 °C and is basically stable at −30 °C and −40 °C. The coefficient of friction of LC2-1/QT350-22L is much lower than that of QT500-7/QT350-22L.

Figure 6b shows the average coefficient of friction of the two sets of friction pairs at different temperatures when the normal force is 30 N. At room temperature, the coefficients of friction of the LC2-1/QT350-22L and QT500-7/QT350-22L are 0.1535 and 0.1885, respectively. With the decrease in temperature, the coefficient of friction of the former also decreases. It stabilizes at about 0.085 at −40 °C. The coefficient of friction of the latter decreases first and then increases at −20 °C. As the temperature decreases from −10 °C to −20 °C, the coefficient of friction increases from 0.1633 to 0.1924. At −40 °C, the coefficient of friction is 0.2017. In short, the coefficient of friction of the friction pair LC2-1/QT350-22L is lower than that of QT500-7/QT350-22L. Meanwhile, the fictional coefficient of the former fluctuates less than does that of the latter under low-temperature conditions. This proves that the friction and wear process is relatively stable.

As shown in Figure 6, comprehensive analyze the change law of oil viscosity and the coefficient of friction, for the friction pair LC2-1/QT350-22L, the variation of the coefficient of friction with temperature complies with the trend of the Stribeck curve. When the temperature drops from 25 °C to −20 °C, the lubrication state between the friction pairs is a mixed or boundary lubrication state. The coefficient of friction is stable when the temperature changes from −30 °C to −40 °C. It is inferred that the lubrication state changes into the mixed or hydrodynamic lubrication state. However, the coefficient of friction variation of QT500-7/QT350-22L does not comply with the trend of the Stribeck curve.

3.3. Wear Volume

The wear scar morphologies of the worn pin samples were observed using CLSM. The diameter of the wear scar was determined by selecting five different directions in the same wear spot circle and averaging the measured values under different test conditions. The measurement schematic diagram is shown in Figure 7a. According to the calculation

schematic diagram shown in Figure 7b, the wear volume is calculated by Equation (2) for the pin wear volume calculation.

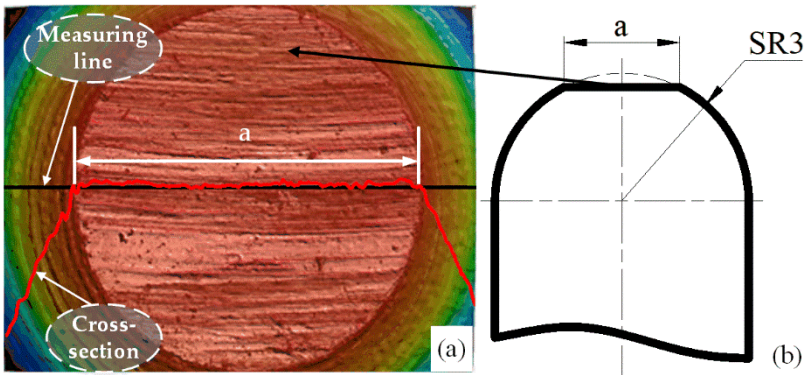

Figure 7. (**a**) Measurement schematic diagram. (**b**) Calculation schematic diagram.

The calculation equation of the wear volume:

$$V = 3\pi * \left(3 - \sqrt{3^2 - \frac{a^2}{4}}\right)^2 - \frac{\pi}{3} * \left(3 - \sqrt{3^2 - \frac{a^2}{4}}\right)^3 \quad (2)$$

In this equation, V is the volume of wear (mm^3); a is the diameter of the wear scar (mm).

If the diameter of the wear scar exceeds 6 mm after the test, Equation (2) for the wear volume calculation cannot be applied, indicating that the friction pair is seriously worn and that the test can be considered a failure. The test should be redone, or the test plan should be reset.

Due to the irregular circular shape of the wear scar, there are errors in the measurement results when the diameter is measured by CLSM. At the same time, because of the different selection of measurement line, it will also lead to measurement error. In the testing process, the average value of the wear scar measurement is taken five times to improve the accuracy of the results.

Figure 8 illustrates that whether the normal force is 20 N or 30 N, the wear volume of LC2-1 and QT500-7 has a similar pattern with temperature. With a drop in temperature, the former's wear volume always reduces. However, as the test temperature goes from room temperature to −10 °C, the wear volume of the latter decreases slightly, then increases abruptly when the test temperature drops to between −10 °C and −20 °C, and then declines steadily between −20 °C and −40 °C.

The wear volume of LC2-1 is decreased from 0.046 to 0.018 mm^3 or a 60% reduction as the temperature lowers from 25 °C to −40 °C and the normal force is 20 N, as illustrated in Figure 8a,b, and the wear volume is lowered from 0.047 to 0.031 mm^3 or a 36% reduction when the normal force is 30 N. The wear volume of the material QT500-7 is reduced from 0.044 to 0.039 mm^3 when the normal force is 20 N and the test temperature is dropped from 25 °C to −10 °C. Then, when the test temperature is −20 °C, its wear volume significantly increases, reaching 0.107 mm^3, which is 3.65 times that of the LC2-1. When the test temperature is −30 °C and −40 °C, the wear volume is 0.09 mm^3 and 0.084 mm^3, respectively, which is 4.0 times and 4.8 times that of the material LC2-1. The wear volume is lowered from 0.058 to 0.039 mm^3 when the load is 30 N, and then increased to 0.125 mm^3 when the temperature swings from −10 °C to −20 °C. At −20 °C, it has 3.4 times the wear volume of the LC2-1. At −30 °C and −40 °C, the wear volume of material QT500-7 is 0.097 mm^3 and 0.094 mm^3, respectively, which is 2.7 times and 3.1 times that of material LC2-1. In addition, the wear volume of QT500-7 is always greater than that of LC2-1. The results prove that the wear resistance of LC2-1 is superior to that of QT500-7.

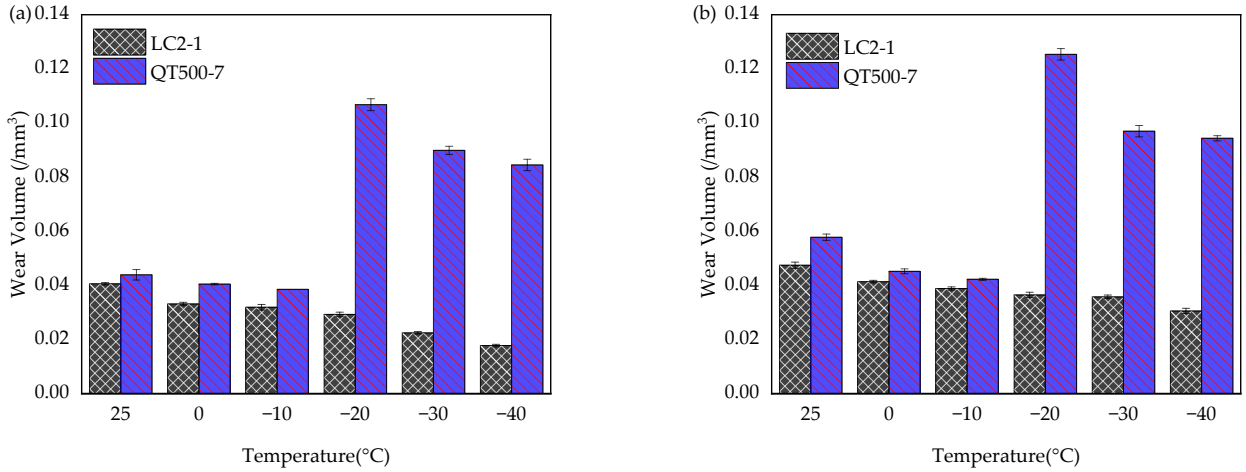

Figure 8. The wear volumes of LC2-1 and QT500-7. (**a**) The wear volumes of LC2-1 and QT500-7 at 20 N. (**b**) The wear volumes of LC2-1 and QT500-7 at 30 N.

Both the coefficient of friction and the wear volume of the two materials are shown in Figures 6 and 8. The coefficient of friction and the wear volume of LC2-1 are larger than their counterparts of QT500-7 under any condition especially when the test temperature is below −20 °C. The results prove that the tribological properties of the former are superior to those of the latter under the test conditions. On the other hand, it can be concluded that the influences of temperature and normal load on the tribological properties of the two materials are inconsistent: the influence of temperature is dominant over the influence of the normal load, largely because temperature not only affects the lubricating characteristics of the lubricating medium, but also changes the mechanical properties of materials. The influence of the low-temperature environment on QT500-7 is more significant than on LC2-1, especially when the ambient temperature drops to around −20 °C.

3.4. Surface Damage

The wear surface of the two kinds of materials under 20 N was observed using SEM to better understand the wear mechanism of the materials, with the results shown in Figure 9. As shown in Figure 9A, the worn surface of LC2-1 is abrasive wear, with wear material accumulating on the worn surface. The reason is that the material has plasticity, hence remaining attached to the sample surface after wear. In Figure 9B,C, the edges of the plough on the worn surface are neater with an amount of small abrasive debris accumulation especially when the temperature drops to −40 °C. This is mainly because the material is brittle at low temperature. Abrasive wear and fatigue wear occur in the material during the friction process, and the wear debris accumulates on the wear surface.

As shown in Figure 9a–c, the wear form of QT500-7 is mainly abrasive wear at room temperature. The result is similar to that of LC2-1. Spalling appears on the worn surface, showing that the form of wear surface is severe fatigue wear when the temperature drops to −20 °C. The ploughs are obvious on the wear surface and there are obvious pitting and spalling when the test temperature drops to −40 °C, indicating that the wear forms are abrasive wear and fatigue wear during the wear process.

By comparing the wear forms of the wear surfaces of the two materials under the same temperature conditions, the difference of the surface damage between the two materials is maximized at the test temperature of −20 °C. The wear surface of LC2-1 is mainly abrasive wear, whereas the surface of QT500-7 has undergone severe fatigue wear. The experiment results are similar to those of scholars [30,31]. The main reason is that the brittle– ductile transition temperature of QT500-7 is between −10 °C and −30 °C.

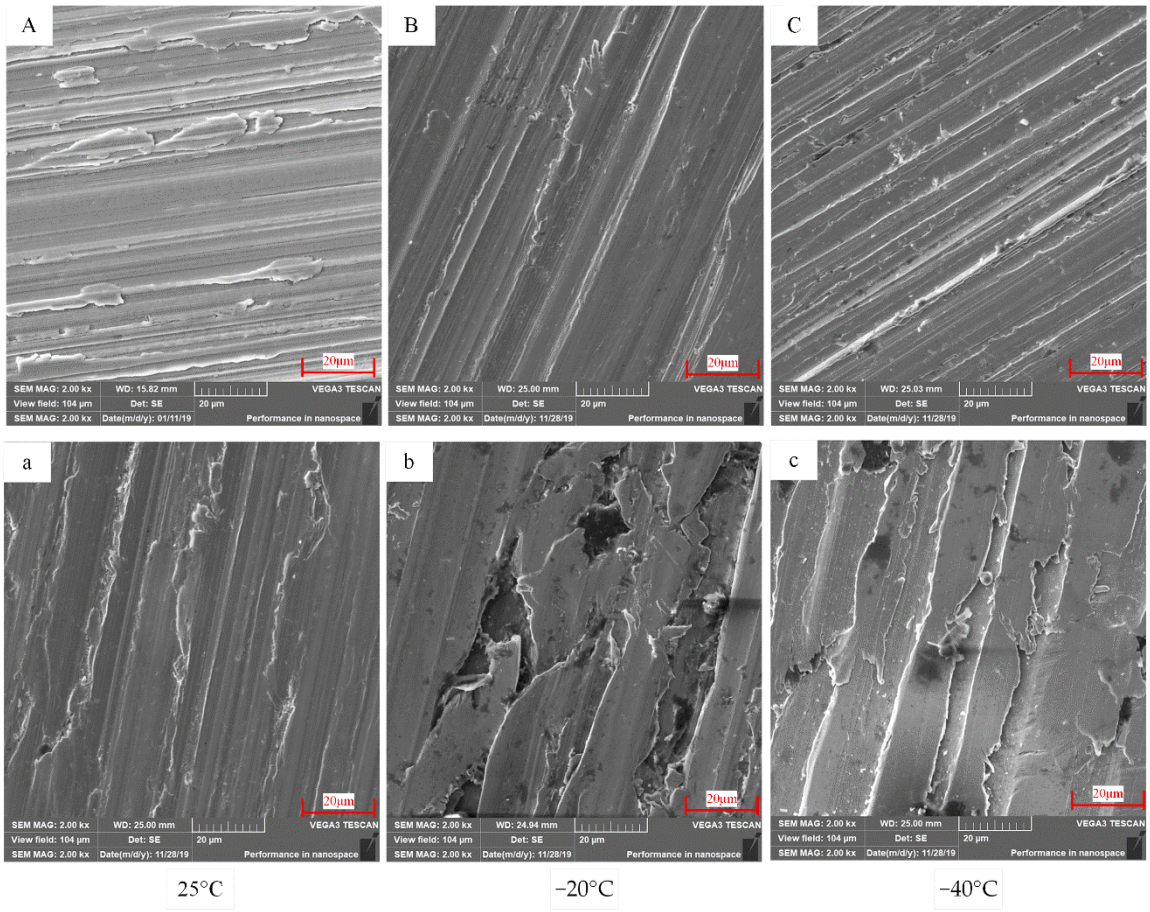

Figure 9. The wear surface morphology of the two material pin samples at different temperatures (**A**–**C**) are the wear surface morphology of LC2-1 when the test temperatures are 25 °C, −20 °C and −40 °C, respectively; (**a**–**c**) are the wear surface morphology of QT500-7 when the test temperatures are 25 °C, −20 °C and −40 °C, respectively.

3.5. Wear Debris

The wear particle morphology was analyzed to provide a powerful basis for judging the form of wear material damage in the wear process and to helpfully infer the wear mechanism between friction pairs. It can be seen from Figure 10 that the size and shape of the wear debris are largely different between LC2-1/QT350-22L and QT500-22L/QT350-22L under the temperature conditions of −20 °C and −40 °C. The wear debris of LC2-1/QT350-22L is similar under the different conditions. The wear debris of the other friction pair was analyzed. When the temperature is −20 °C, there is wear debris with a size of about 100 μm × 40 μm and with irregularly torn edges. Moreover, there are obvious wear marks and holes in its surface. The results indicate that the friction pair has peeled off during the wear process, and that the peeled material has entered into the friction pair, causing serious damage to the friction pair material. When the temperature drops to −40 °C, the wear debris is still irregularly shaped, and the size of the wear debris is about 60 μm × 40 μm. This shows that the friction pair has also undergone material peeling. However, as the temperature varies from −40 °C to −20 °C, the degree of wear of the material decreases due to the smaller size of the wear debris.

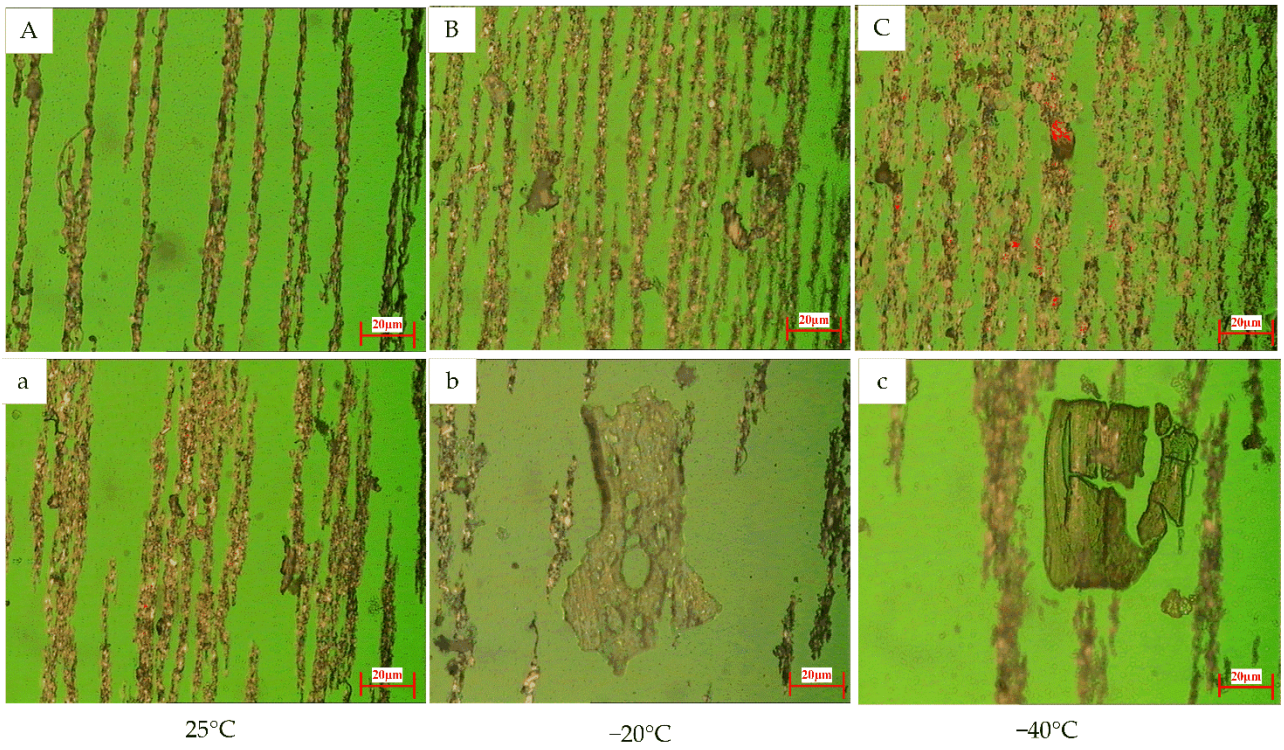

Figure 10. Morphology of abrasive grains of the friction pairs of the two materials at different temperatures. (**A**–**C**) are morphology of abrasive grains of the friction pair of LC2-1 with QT350-22L when the test temperatures are 25 °C, −20 °C and −40 °C, respectively; (**a**–**c**) are morphology of abrasive grains of the friction pair of QT500-7 with QT350-22L when the test temperatures are 25 °C, −20 °C and −40 °C, respectively.

Through comparison of the wear debris morphology between the two sets of friction pairs, it can be seen that QT500-7/QT350-22L has various forms of wear and that severe material peeling occurs at low-temperature environments. The degree of wear is more serious than that of LC2-1/QT350-22L. The wear debris size of the former is much larger especially when the test temperature is below −20 °C.

4. Discussion

Combining the coefficient of friction, wear volume, and surface morphology of the two types of pin samples, the shape and size of wear debris are comprehensively analyzed in various temperature tests. Each test result of the QT500-7 test ground increased when the material was exposed below −20 °C. According to the experimental results, the impact energy of the material has an effect on its tribological properties. The impact energy of QT500-7 decreases sharply between −10 °C and −30 °C, and its change rate is bigger than that of LC2-1, (as shown in Figure 5). The fatigue wear of materials is aggravated at this test temperature, so the tribological properties are the worst, and the wear damage is more serious. When the temperature is −30 °C or −40 °C, the brittleness of the material increases so that the surface of the material is prone to fatigue and wear and is vulnerable to serious damage. From the shape and size of wear debris, it can be inferred that the wear debris has entered the friction pair again, causing the friction pair to undergo "three-body" wear, which in turn aggravates material wear. During this wear process, the hydraulic oil film is destroyed, and the lubrication performance of the hydraulic oil worsens.

Based on the above analysis, the material LC2-1 with stable wear performance is more applicable for being processed and manufactured into parts for low-temperature environmental conditions, as there is no serious fluctuation in the temperature range from −40 °C to room temperature. Therefore, it is imperative to explore the wear mechanism of LC2-1/QT350-22L at different temperatures.

Figure 11 shows the morphology of the unworn and worn surfaces of the disc paired with LC2-1 at different test temperatures. The normal load is 20 N and the rotary speed is 300 r·min^{-1} in these tests. The left part of each picture is the original unworn surface morphology of the disc samples, and the right part is the worn surface morphology of the disc samples. As shown in Figure 11, when the test temperature is room temperature (25 °C), there is obvious deformation at the edges of the wear mark. This is due to the ductility of QT350-22L and the fact that the wear debris is only partially separated from its body. In addition, there are some ploughs on the worn surface, a morphological feature of abrasive wear. At the test temperature of −20 °C, the worn surface has uniform, fine and shallow ploughs. The edges of the wear marks are neatly accompanied by the accumulation of material, except for the only difference that the wear debris is inlaid in the ploughs, indicating the existence of "three-body" abrasive wear. As the test temperature drops to −40 °C, the wear edge is still neat but there is no obvious accumulation. The most remarkable thing is that there are traces of material peeling off the edges. This is mainly due to the brittleness of the material increasing with the decrease in temperature. The wear debris leaves the body, and the material appears slight fatigue wear.

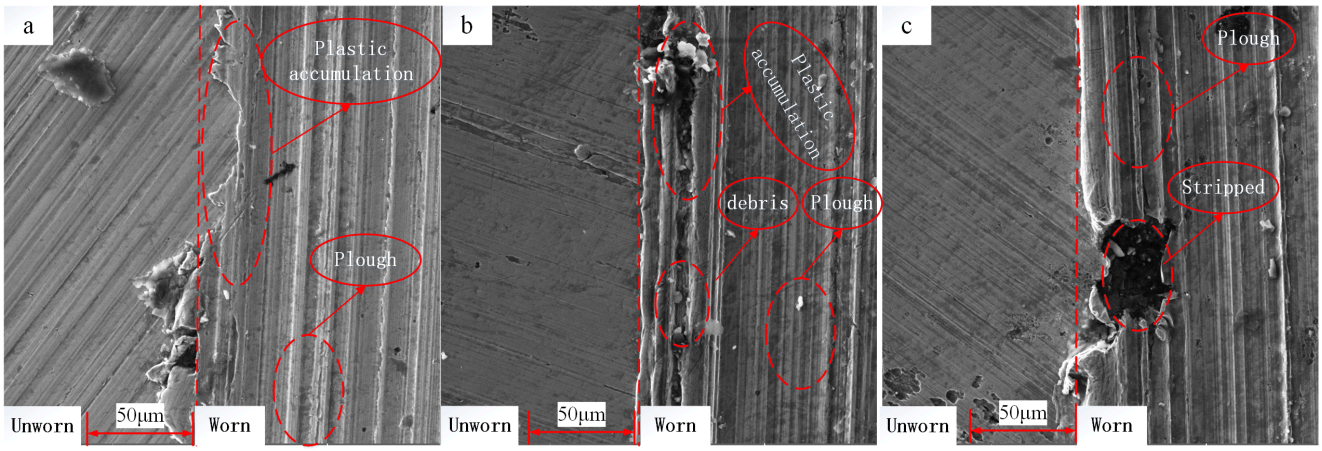

Figure 11. The surface morphology of QT350-22L sliding contact with LC2-1. (**a**) 25 °C; (**b**) −20 °C; (**c**) −40 °C.

To sum up, Figure 12 shows a schematic diagram of the wear process of the friction pair during sliding under the certain normal force (F) and rotational speed (ω) conditions. The friction pair material is immersed in hydraulic oil. When the disc rotates, the hydraulic oil enters the friction pair to form a certain fluid dynamic pressure, hence a certain thickness of oil film acting as the lubricant. The lower the test temperature, the larger the oil viscosity, hence the worse fluidity of the hydraulic oil, and the higher dynamic pressure generated by the fluid between the friction pairs. A thicker oil film can be formed, and the lubrication effect is better. However, the wear debris may not be brought out in time and re-enter the friction pair to form "three-body" wear.

There is another issue that needs to be considered. The mechanical properties of the material also affect the friction and wear during the wear process at different test temperatures. At room temperature, the material exhibits excellent plasticity, and the wear debris tends to accumulate on the wear surface. As the temperature drops, the brittleness of the material increases. Then, the material peels off on the wear surface. The effect is that it is easier for the material to wear during sliding. The wear becomes serious when the material undergoes a fatigue wear.

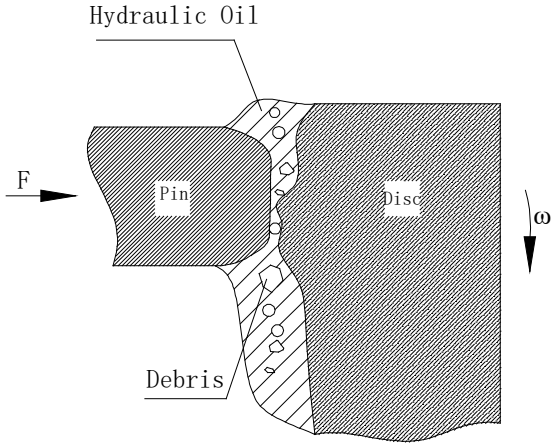

Figure 12. Schematic diagram of the lubrication and wear process.

5. Conclusions

In the present study, the viscosity of hydraulic oil and the impact strength of the two materials were measured via viscometer and mechanical bench. The tribological properties of the two typical materials of hydraulic motor's rotor were analyzed at different ambient temperatures, especially at low temperature. A series of tribological experiments were performed to explore the wear process and mechanism of two sets of friction pairs. and to select the suitable material for the rotor. There are some conclusions drawn as follows.

(i) Temperature has a significant effect on material properties and the viscosity of lubricating oil. The viscosity gradient increases with temperature dropping. As the test temperature drops from 25 to −40 °C, the viscosity of hydraulic oil increases from 15.96 to 263.27 mPa·s. The viscosity gradient increases with temperature dropping. The minimum gradient of oil viscosity with temperature is 0.71 mPa·s/°C when the test temperature ranges from 25 °C to 0 °C. The viscosity of hydraulic oil is 147.73 to 263.27 mPa·s when the temperature drops from −30 °C to −40 °C, and there is the maximum viscosity gradient and it is 11.95 mPa·s/°C. The viscosity gradient is increased by about 16.8 times. The impact energy of the two types of materials decreases as the temperature decreases. However, the variation trend of the impact energy of LC2-1 is not as obvious as that of QT500-7. For the material QT500-7, there are two consecutive subintervals of sharp decreases from 97.3 J to 42.2 J and then to 18.0 J as the temperature drops from −10 °C to −20 °C and then to −30 °C. The percentage decreases are −56.6% and −57.3%, respectively. It is worth mentioning that the brittle–ductile transition temperature of QT500-7 is between −10 °C and −30 °C.

(ii) Each test result of the QT500-7 ground test is worse when the tribological experiments are carried out at −20 °C. There is a maximum difference of around −20 °C. The wear volume of material QT500-7 sharply increases and reaches the maximum of 0.107 mm^3 when the normal force is 20 N, which is 3.65 times as much as the wear volume of the LC2-1. When the normal force is 30 N, the wear volume of material QT500-7 and LC2-1 are 0.125 and 0.036 mm^3, respectively. The wear volume of former is 3.4 times that of the latter. The results indicate that the impact energy of the material affect its tribological properties since the impact energy of the material QT500-7 decreases sharply at the temperature of −10 to −30 °C.

(iii) Under low-temperature conditions, both materials experience fatigue wear while sliding with QT350-22L, indicating that the low-temperature environment will accelerate the fatigue of the material, but the temperature at which fatigue wear occurs differs from material to material. The material QT500-7 undergoes severe fatigue wear all over its surface at −20 °C, whereas LC2-1 has insignificant fatigue wear at −40 °C. This is mainly because QT500-7 has a ductile–brittle transition between

−10 °C and −30 °C such that the wear is most serious. However, LC2-1 has no obvious ductile–brittle transition within the test temperature range.

(vi) The wear resistance of LC2-1 in a low-temperature environment is superior to that of QT500-7. The friction pair composed of LC2-1 with QT350-22L has better tribological characteristics. The material LC2-1 with stable wear performance is more applicable for being processed and manufactured into parts for low-temperature environmental conditions, as there is no serious fluctuation in the temperature range from −40 °C to room temperature.

This paper considers only the hydraulic oil viscosity changes with constant temperature and the influence of the friction pair material, limited experimental conditions and testing equipment, not directly by effective means of detection in the process of friction and wear test medium oil film thickness changes. The future research will attempt to use an appropriate test method to observe the changing process of the oil film. In addition, the influence process and mechanism of low temperature on mechanical properties of materials need to be further analyzed and studied.

Author Contributions: Conceptualization, G.W. and M.T.; methodology, G.W.; software, G.W. and M.L.; validation, G.W. and K.Y.; formal analysis, G.W. and K.Y.; investigation, G.W.; resources, G.W; data curation, G.W.; writing—original draft preparation, G.W. and M.L.; writing—review and editing, G.W., M.T. and Q.W.; visualization, Q.W.; supervision, G.W.; project administration, M.T.; funding acquisition, G.W. and M.L. All authors have read and agreed to the published version of the manuscript.

Funding: This research was supported by the National Natural Science Foundation of China (grant number. 52101372), Post-doctoral Independent Innovation Foundation of Wuhan University of Technology (No: 203305001) and Open Research Fund of National and Local Joint Engineering Research Center of Industrial Friction and Lubrication Technology.

Institutional Review Board Statement: Not applicable.

Informed Consent Statement: Not applicable.

Data Availability Statement: Not applicable.

Conflicts of Interest: The authors declare no conflict of interest. The funders had no role in the design of the study; in the collection, analyses, or interpretation of data; in the writing of the manuscript, or in the decision to publish the results.

References

1. Theocharis, D.; Pettit, S.; Rodrigues, V.S.; Haider, J. Arctic shipping: A systematic literature review of comparative studies. *J. Transp. Geogr.* **2018**, *69*, 112–128. [CrossRef]
2. Zhu, Y.F.; Liu, Z.Y.; Xie, D.; Li, W.H. Advancements of the core fundamental technlogies and strategies of China regarding the research and devo lopment on polar ships. *China Sci. Found.* **2015**, *29*, 178–186.
3. Zheng, F.; Lv, M.; Wang, Q.H.; Wang, T.M. Effect of temperature on friction and wear behaviors of polyimide (PI)-based solid-liquid lubricating materials. *Polym. Adv. Technol.* **2015**, *26*, 988–993. [CrossRef]
4. Wang, Q.H.; Zheng, F.; Wang, T.M. Tribological properties of polymers PI, PTFE and PEEK at cryogenic temperature in vacuum. *Cryogenics* **2016**, *75*, 19–25. [CrossRef]
5. Duan, Z.B.; Zhang, S.L.; Wang, S.S.; Li, R.Z. Research on visco-temperature characteristics of turbine oil. *Procedia Eng.* **2017**, *174*, 246–250. [CrossRef]
6. Liu, H.C.; Zhang, B.B.; Bader, N.; Guo, F.; Poll, P.; Yang, P. Crucial role of solid body temperature on elastohydrodynamic film thickness and traction. *Tribol. Int.* **2019**, *131*, 386–397. [CrossRef]
7. Cai, Z.B.; Zhou, Y.; Qu, J. Effect of oil temperature on tribological behavior of a lubricated steel−steel contact. *Wear* **2015**, *332–333*, 1158–1163. [CrossRef]
8. Bergada, J.M.; Kumar, S.; Davies, D.L.; Watton, J. A complete analysis of axial piston pump leakage and output flow ripples. *Appl. Math. Model.* **2012**, *36*, 1731–1751. [CrossRef]
9. Tang, H.; Ren, Y.; Xiang, J. A novel model for predicting thermoelastohydrodynamic lubrication characteristics of slipper pair in axial piston pump. *Int. J. Mech. Sci.* **2017**, *124–125*, 109–121. [CrossRef]
10. Wang, Y.S.; Cao, J.W.; Li, H.; Li, P. Study of frictional and viscosity-temperature characteristics of a space lubricating oil No. 4129 in rolling/sliding contact. *Acta Armamentarii* **2014**, *9*, 1515–1520.

11. Gu, K.; Zhang, H.; Zhao, B.; Wang, J.J.; Zhou, Y.; Li, Z.Q. Effect of cryogenic treatment and aging treatment on the tensile properties and microstructure of Ti-6Al-4V alloy. *Mater. Sci. Eng. A* **2013**, *584*, 170–176. [CrossRef]
12. Yan, J.B.; Xie, J. Experimental studies on mechanical properties of steel reinforcements under cryogenic temperatures. *Constr. Build. Mater.* **2017**, *15*, 661–672. [CrossRef]
13. Kim, M.J.; Kim, S.; Lee, S.K.; Kim, J.H.; Lee, K.; Yoo, D.Y. Mechanical properties of ultra-high-performance fiber-reinforced concrete at cryogenic temperatures. *Constr. Build. Mater.* **2017**, *157*, 498–508. [CrossRef]
14. Tong, W.P.; Sun, J.; Zuo, L.; He, J.C.; Lu, J. Study on wear and friction resistance of nanocrystalline Fe nitrided at low temperature. *Wear* **2011**, *271*, 653–657. [CrossRef]
15. Wan, G.; Wu, Q.; Yang, K. Tribological properties of the vane head/stator of hydraulic vane motor in the low ambient temperature. *Tribol. Int.* **2020**, *149*, 105570. [CrossRef]
16. Zheng, C.S.; Yu, W.W. Effect of low-temperature on mechanical behavior for an AISI 304 austenitic stainless steel. *Mater. Sci. Eng. A* **2018**, *710*, 359–365. [CrossRef]
17. Mallick, P.; Tewary, N.K.; Ghosh, S.K.; Chattopadhyay, P.P. Effect of cryogenic deformation on microstructure and mechanical properties of 304 austenitic stainless steel. *Mater. Charact.* **2017**, *133*, 77–86. [CrossRef]
18. Yang, H.S.; Wang, J.; Shen, B.L.; Liu, H.H.; Gao, S.J.; Huang, S.J. Effect of cryogenic treatment on the matrix structure and abrasion resistance of white cast iron subjected to destabilization treatment. *Wear* **2006**, *261*, 1150–1154. [CrossRef]
19. Xie, J.; Zhao, X.Q.; Yan, J.B. Mechanical properties of high strength steel strand at low temperatures: Tests and analysis. *Constr. Build. Mater.* **2018**, *189*, 1076–1092. [CrossRef]
20. Xiao, X.; Xiao, H. Autonomous robotic feature-based freeform fabrication approach. *Materials* **2021**, *15*, 247. [CrossRef]
21. Ceschini, L.; Chiavari, C.; Lanzoni, E.; Martini, C. Low-temperature carburised AISI 316L austenitic stainless steel: Wear and corrosion behaviour. *Mater. Des.* **2012**, *38*, 154–160. [CrossRef]
22. Hübner, W.; Gradt, T.; Schneider, T.; Borner, H. Tribological behaviour of materials at cryogenic temperatures. *Wear* **1998**, *216*, 150–159. [CrossRef]
23. Siva, S.R.; Mohan, L.D.; Kesavan, N.P.; Arockia, J.M. Influence of cryogenic treatment on the wear characteristics of 100Cr6 bearing steel. *Int. J. Miner. Metall. Mater.* **2014**, *21*, 46–51. [CrossRef]
24. Jaswin, M.A.; Shankar, G.S.; Lal, D.M. Wear resistance enhancement in cryotreated En 52 and 21-4N valve steels. *Int. J. Precis. Eng. Manuf.* **2010**, *11*, 97–105. [CrossRef]
25. Kennedy, F.E.; Lu, Y.; Baker, I. Contact temperatures and their influence on wear during pin-on-disk tribotesting. *Tribol. Int.* **2015**, *82*, 534–542. [CrossRef]
26. Wang, D.S.; Chang, X.T.; Wang, S.Y.; Sun, S.B.; Yin, Y.S. Friction and wear properties of 10CrMn2NiSiCuAl icebreaker steel plates effected by temperature. *J. Chongqing Univ.* **2018**, *41*, 66–75, 90.
27. Wang, D.S.; Wang, S.Y.; Sun, S.B.; Chang, X.T.; Yin, Y.S. Dry friction performance of novel polar marine icebreaker steel plate. *Mater. Prot.* **2017**, *50*, 24–27.
28. Wang, H.L.; Yan, F.Y. Study on tribological behavior of 1.08%C steel under dry friction at low temperature. *Tribology* **2008**, *28*, 469–474.
29. Ma, L.; Shi, L.B.; Guo, J.; Liu, Q.Y.; Wang, W.J. On the wear and damage characteristics of rail material under low temperature environment condition. *Wear* **2018**, *394–395*, 149–158. [CrossRef]
30. Ma, L.; Wang, W.J.; Guo, J.; Liu, Q.Y. Study on wear and fatigue performance of two types of high-speed railway wheel Materials at Different Ambient Temperatures. *Materials* **2020**, *13*, 1152. [CrossRef]
31. Polar Ship Guide. 2016. Available online: https://www.ccs.org.cn/ccswz/articleDetail?id=201900001000005807 (accessed on 10 May 2022).
32. Wan, G.; Wu, Q.; Yan, X.P.; Yang, K. Tribological properties of the plate valve and rotor material of hydraulic vane motor on different ambient temperature. *Wear* **2019**, *426–427*, 887–895. [CrossRef]